Characteristics and dynamics of crescentic bar events at Castelldefels beach.

Características y dinámica de los eventos de barras crescénticas en la playa de Castelldefels.

R. L. de Swart[1], F. Ribas[1], G. Simarro[2], J. Guillén[2]

1 Dpt. Física, Universitat Politècnica de Catalunya, c/ Jordi Girona 1-3, 08034 Barcelona. rinse.de.swart@upc.edu, francesca.ribas@upc.edu
2 Dpto. Geociencias Marinas, Institut de Ciències del Mar (ICM-CSIC), Barcelona. simarro@icm.csic.es, jorge@icm.csic.es

Abstract: Crescentic sand bars have been studied intensively in the last decades, resulting in good knowledge of some of their characteristics, but the processes behind their formation and destruction are not yet clear. This study aims to increase our understanding of the dynamics of crescentic bars at an open, dissipative Mediterranean beach (Castelldefels, 20 km southwest of Barcelona). Their dynamics have been analysed using a 4.25-year dataset of video images. The crescentic bar events have been identified using visual analysis, including the formation and destruction moments. The results show that crescentic bars hardly occurred when the sandbar was located close to the beach, whilst they developed often when the sandbar was further offshore. Wave conditions during crescentic bar formation were low- to intermediate-energy waves with both oblique and shore-normal angles of incidence. Sandbar straightening was preferably observed for oblique waves (of both intermediate and high energy). The alongshore wavelength and cross-shore amplitude of the crescentic bars have been also quantified, giving some 245 m and 10 m on average, respectively.

***Key words*:** nearshore morphodynamics, Castelldefels beach, video observations, crescentic bars.

Resumen: *Las barras de arena crescénticas de la zona costera se han estudiado intensamente durante las últimas décadas adquiriendo un buen conocimiento de algunas de sus características, aunque los procesos responsables de su formación y destrucción aún no están claros. El objetivo de este estudio es mejorar nuestra comprensión de la dinámica de las barras crescénticas en una playa mediterránea abierta y disipativa (Castelldefels, a 20 km al suroeste de Barcelona). Se han utilizado datos obtenidos de imágenes de vídeo durante 4.25 años. Los eventos de barras crescénticas, incluidos los momentos de formación y destrucción, se han identificado mediante análisis visual. Los resultados muestran que estos patrones apenas ocurrieron cuando la barra estaba muy cerca de la línea de costa, mientras que se desarrollaron a menudo cuando la barra estaba más alejada. Las condiciones de oleaje durante la formación de barras crescénticas eran de energía baja o intermedia, con ángulos de incidencia tanto oblicuos como normales. Su destrucción se observó preferentemente durante oleajes oblicuos (de energía intermedia o alta). También se han cuantificado la longitud de onda a lo largo de la costa y la amplitud transversal de las barras crescénticas, dando un promedio de 245 m y 10 m, respectivamente.*

Palabras clave: *morfodinámica de costas, playa de Castelldefels, video-observaciones, barras crescénticas.*

INTRODUCTION

The nearshore zone of beaches often features one or several shore-parallel sand bars, where incoming waves predominately break. These bars can be alongshore uniform or alongshore variable. Crescentic bars are characterised by regular undulating sequences of shallow areas (horns) and deeper regions (bays; Van Enckevort et al., 2004). Nowadays, it is widely accepted that these patterns develop due to a self-organization process (Ribas et al., 2015) that cause a positive feedback between the currents and the morphology (Calvete et al., 2005).

Crescentic sand bars have been studied intensively in the past, resulting in good knowledge of some of their characteristics (Van Enckevort et al., 2004; Price and Ruessink, 2011). However, the processes behind crescentic bar formation and destruction are not yet clear and deserve further attention. Traditionally, the transitions from a shore-parallel bar to a crescentic bar and vice versa were associated to the amount of incoming wave energy, with bar straightening occurring for high energy waves (e.g. van Enckevort et al., 2004). However, more recent studies (e.g. Price and Ruessink, 2011) indicated that crescentic bars primarily develop for normal wave incidence and bar straightening occurs during obliquely incident waves.

Still, the role of wave obliquity in crescentic bar formation and destruction is not clear. In addition, there is a lack of crescentic bar observations in fetch-limited areas with insignificant tides, where waves are the only existing morphodynamic forcing, such as Mediterranean beaches. This paper aims to further our

understanding of the dynamics of crescentic bars (including their straightening) at Mediterranean beaches. This will be done by using a 4.25 years-long dataset of daily high-quality video images from Castelldefels beach, Catalunya, Spain. After explaining the methods used to characterise the crescentic bar events, their characteristics will be quantified and correlated to the wave conditions, paying special attention to their formation and destruction.

STUDY AREA AND DATA COLLECTION

Study area

The study site is Castelldefels beach, an open, dissipative beach located approximately 20 km southwest of Barcelona (Northeast Spain), at the North-western Mediterranean Sea. Tidal action in this part of the Mediterranean Sea is very small, with a tidal range of approximately 20 (10) cm during spring tide (neap tide). Castelldefels beach is part of a continuous stretch of beaches of the Llobregat delta, extending from the Garraf Mountain chain in the west to the Llobregat river outfall in the east. The orientation of the studied part of Castelldefels beach is east-west and extends over an alongshore distance of 1 km. The sand at the beach has a median grain size of 270 μm.

Morphological data

A video monitoring system operates at Castelldefels beach since 5 October 2010. It is installed in a 30-m-high observation tower and uses the SIRENA open source code (Nieto et al., 2010). Each daylight hour, the cameras produce one snapshot, one time-exposure and one variance image. Each time-exposure image shows clear stripes of foam, which indicate the location of the submerged sand bars. Finally, the time-exposure images from the 5 cameras are georeferenced, rectified and merged into a planview with a size of 1000 by 300 m (Figure 1) using the ULISES open source code (Simarro et al., 2017). The origin of the coordinate system in the planviews is the location of the camera system (41°15'54.7"N, 1°59'29.1"E). The time period studied in the present contribution spans from 5 October 2010 to 31 December 2014. During this period of 1549 days, a nearly uninterrupted dataset of images is available with only 69 days without images.

Wave data

For this study, hourly values of the root-mean-square wave height H_{rms}, peak period T_p and incidence angle θ_{mean} were obtained from the SIMAR model point 2108135, located in front of the study site at 21 m depth. The waves were propagated to a depth of 10 m using Snell's law, dispersion relation and wave energy conservation (linear wave theory). The angle of incidence is defined with respect to the shore normal, where positive (negative) angles indicate that waves come from the west (east).

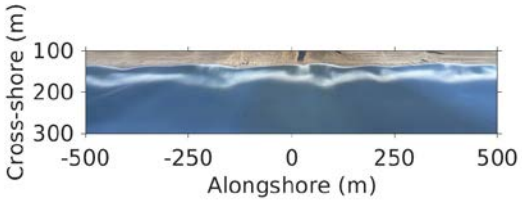

FIGURE 1. *Planview of 10 June 2013 (11h) made of 5 time-exposure vídeo images. The dry beach is in the upper part and white stripes (due to predominant wave breaking) correspond to shallow areas.*

The beach of Castelldefels is exposed to waves throughout the year. The long-term average values of H_{rms}, T_p and absolute θ_{mean} during the entire study period (at 10 m depth) are 0.32 m, 4.4 s and 35° respectively. Higher than average wave heights are mostly observed between September and March, corresponding to the autumn and winter period. The wave climate at Castelldefels is characterised by waves from both the East-Southeast and the Southwest, with the highest waves coming from the East (Sánchez-Arcilla et al., 2008).

METHODS

During the entire study period, a visual analysis of the planviews was performed that focused on tracking the visibility of the inner and outer bar, and also the occurrence of crescentic bar events. A crescentic bar event was defined when at least 2 undulations could be visually distinguished for at least one full day (see Figure 1 for an example). Moreover, the formation moments were defined when the first clear crescentic pattern was visible in the planview images, following a period with only shore-parallel bars. Similarly, destruction moments were defined when a crescentic pattern was not visible anymore in the planview images, following a period with only crescentic bars.

The barlines in the planview images were also tracked using the BarLine Intensity Mapper (BLIM), a tool which detects the maximum intensity value in a cross-shore transect. Normally, one planview per day was selected to quantify the bar characteristics. When large changes in the wave breaking pattern were observed on the same day, up to three images per day were used. Days with only low-quality images or without a clear wave breaking pattern were discarded. For each selected image, the cross-shore location of the maximum intensity was inferred for each alongshore location using BLIM, resulting in smoothed barlines for all images in the dataset. For each barline, the average cross-shore location was computed.

Next, crescentic bars were detected in each barline by identifying the bays and horns. Subsequently, the wavelength and amplitude of each crescentic bar were computed using the method of Van Enckevort et al. (2004). Finally, alongshore migration rates were computed for sequences of at least 3 days with crescentic bars by cross-correlating the bar crest lines of the first and last day of the sequence. The migration distance is equivalent to the largest positive magnitude

of the lag, located closest to the origin of the cross-correlogram. The sign of the lag depicts the direction of the migration (positive for eastward migration). A minimum correlation of 0.6 between the images was imposed, so that migration rates between images with limited correlation were discarded.

RESULTS

Crescentic bar occurrence

During the study period (Oct 2010 – Dec 2014), a total of 41 crescentic bar events were observed in the inner bar whilst the outer bar was always alongshore uniform. In total, crescentic bars were observed during 41% of the time. No clear seasonal signal was present in the manifestation of crescentic bars but their presence was uneven in different years. The majority of the events occurred during Oct 2010 – Mar 2011 and Jan 2013 – Dec 2014 (Figure 2, top). The duration of the events is longer in 2010, 2013 and 2014, with an event in 2013 lasting nearly one-third of the entire year.

The sharp contrast in crescentic bar occurrence between the period Apr 2011 – Dec 2012 and the rest of the studied period turns out to be related with a change in the shore-parallel cross-shore bar location (Figure 2, bottom). In Oct 2010 – Dec 2010, an inner bar (bar 1) was located approximately 50 m of the shoreline ($B_y \approx 200$ m; the shoreline position was located at about 150 m across the whole study period). In February 2011, a new inner bar (bar 2) appeared very close to the shoreline and bar 1 moved slightly seaward. In May 2011, bar 1 migrated offshore and disappeared from from our analysis. From May 2011 – February 2013, bar 2 was located very close to the shore (< 30 m from the shoreline, which corresponds to $B_y < 180$ m), and only a few isolated crescentic bar events occurred. However, in March 2013 bar 2 migrated offshore to $B_y \approx 200$ m, at about 50 m from the shoreline, and crescentic bars were mostly present for the remainder of the study period.

Crescentic bar characteristics

Most crescentic bars occurred during 2013 and 2014, thus a detailed analysis of the bar characteristics was carried out for these two years (Figure 3). Large variability is observed for wavelength L_y, which ranges from approximately 100 to over 400 m. The amplitude A_y ranges from 3 to 18 m. For most of the time, the alongshore migration rates C_y did not exceed 2 m/day.

The temporal development of crescentic bar events during 2013 and 2014 at Castelldefels beach showed more or less the same pattern. Pre-existing crescentic bars were often wiped out during high energetic oblique wave conditions and as a result B_y moved offshore by approximately 10 – 20 m. A few days after the storm, the first crescentic bars appeared with low amplitudes ($A_y < 10$ m) and large wavelengths ($L_y >$ 300 m). In the course of time, new crescents developed between the already existing ones, causing L_y to decrease to 100 – 200 m. During the remaining lifetime,

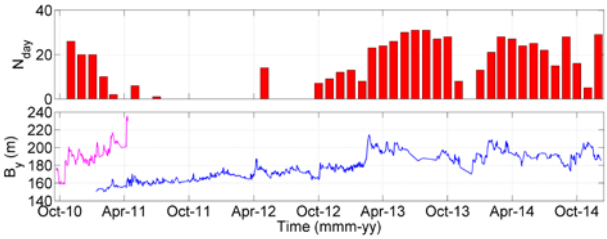

FIGURE 2. *The number of days per month with crescentic bar events at Castelldefels (top) and the alongshore-averaged sandbar position B_y (bottom) during the entire study period (shoreline position was located around 150 m). The pink line in the lower panel is related with bar 1 and the blue line with bar 2.*

L_y varied significantly (due to splitting and merging of individual crescents), whilst A_y was mostly quite constant. Throughout each long-lived event, the bar generally migrated onshore (typical rates of 0.5 – 1 m/day). Often, a next storm wiped out the crescentic shapes and forced the bar offshore again.

Crescentic bar formation and destruction

During the study period, daily-averaged H_{rms} varied from 0.1 to 1.5 m, T_p from 2.5 to 11 s, and absolute values of θ_{mean} from 0 to 86° (at 10 m depth). Easterly waves were dominant (63% of the time) over westerly waves. Crescentic bars are mostly observed in low-energetic conditions ($H_{rms} < 0.85$ m and $T_p < 7.5$ s) with waves coming from the East.

The wave conditions prior to formation and during destruction of crescentic bars were analysed by averaging over the 24 hours prior to a formation (destruction) moment. During the day prior to crescentic bar observation, H_{rms} never exceeded 0.8 m, with an average value of 0.4 m, and absolute values of θ_{mean} varying from 3 to 81°, with an average value of 33°. An equal dominance was observed for waves from easterly and westerly directions, but the angle of incidence was less oblique compared to the entire dataset. The wave conditions during destruction moments are more energetic (average H_{rms} increases to 0.6 m) with storms also well represented. Nevertheless, crescentic bar destruction also occurred in low-energy wave conditions ($H_{rms} < 0.4$ m). The dominant wave direction was West (58% of the time, whilst most waves in the entire dataset came from the East), with most destruction moments taking place during oblique waves of intermediate to large wave height. All this underlines the important role of oblique waves in crescentic bar destruction.

CONCLUSIONS

During a study period of 4.25 years (October 2010 – December 2014), a large variability in crescentic bar occurrence is observed at Castelldefels, an open Mediterranean beach with limited tidal action. Many crescentic bar events are observed during 2010, 2013 and 2014 which often last longer than one month. In contrast, relatively few crescentic bar events with short duration occur in 2011 – 2012. The crescentic bars

during 2013 and 2014 show a large variety in wavelength (100–400 m, due to splitting and merging of crescents), whilst the amplitude (range 5–20 m) and alongshore migration rate (1 m/day) are less variable.

At Castelldefels, crescentic bars develop mostly during periods with low-energy wave conditions and both oblique and shore-normal waves. Apart from that, the bathymetric configuration also plays an important role. Crescentic bars only develop when the sand bar is located at least 50 m from the shoreline, they are hardly observed when the sandbar is located closer to the beach. The observations at Castelldefels show that crescentic bar destruction occurs both in low and high-energy wave conditions. However, bar straightening is only observed for oblique waves, confirming the important role of the wave angle in crescentic bar destruction that has been observed in other sites.

ACKNOWLEDGEMENTS

This work has been funded by the Spanish government through the research projects CTM2015-66225-C2-1-P and CTM2015-66225-C2-2-P (MINECO/FEDER). We thank Puertos del Estado for providing the wave data used in this study.

REFERENCES

Calvete, D., Dodd, N., Falqués, A. and Van Leeuwen, S.M. (2005): Morphological development of rip channel systems: Normal and near-normal wave incidence. *Journal of Geophysical Research: Oceans*, 110(C10).

Nieto, M.A., Garau, B., Balle, S., Simarro, G., Zarruk, G.A., Ortiz, A., Tintoré, J., Álvarez-Ellacuría, A., Gómez-Pujol, L. and Orfila, A. (2010): An open source, low cost video-based coastal monitoring system. *Earth Surface Processes and Landforms*, 35(14): 1712-1719.

Price, T.D., and Ruessink, B.G. (2011): State dynamics of a double sandbar system. *Continental Shelf Research*, 31(6): 659-674.

Ribas, F., Falqués, A., Swart, H.E., Dodd, N., Garnier, R. and Calvete, D. (2015): Understanding coastal morphodynamic patterns from depth-averaged sediment concentration. *Reviews of Geophysics*, 53: 362–410.

Sánchez-Arcilla, A., González-Marco, D. and Bolaños, R. (2008): A review of wave climate and prediction along the Spanish Mediterranean coast. *Nat. Hazards Earth Syst. Sci*, 8: 1217-1228.

Simarro, G., Ribas, F., Álvarez, A., Guillén, J., Chic, Ò. and Orfila, A. (2017): Ulises: An open source code for extrinsic calibrations and planview generations in coastal video monitoring systems. *Journal of Coastal Research*, 33(5), 1217-1227.

Van Enckevort, I.M.J., Ruessink, B.G., Coco, G., Suzuki, K., Turner, I.L., Plant, N.G., and Holman, R.A. (2004): Observations of nearshore crescentic sandbars. *Journal of Geophysical Research: Oceans*, 109(C6).

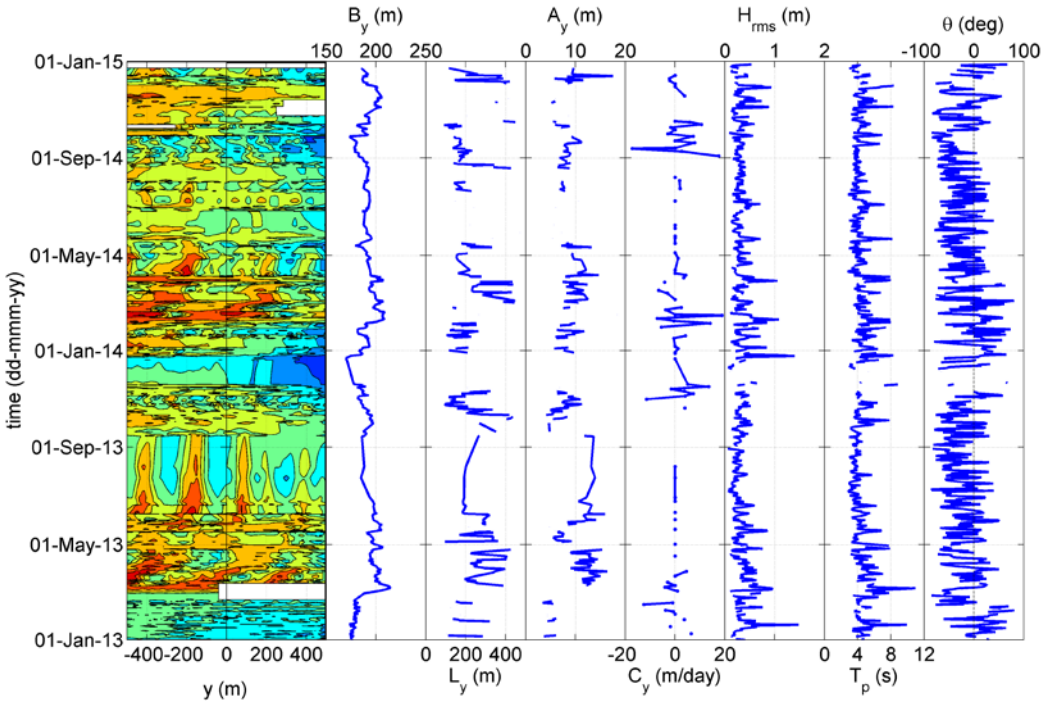

FIGURE 3. *Time series during 2013-2014 of (from left to right) the cross-shore bar crest positions B(y,t) (timestack), sandbar position B_y (shoreline position was located around 150 m), wavelength L_y, amplitude A_y, alongshore migration speed C_y (positive for eastward migration), root-mean-square wave height H_{rms}, peak period T_p and angle of incidence θ_{mean} with respect to the shore normal (positive angles are westerly wave). In the timestack, red colours denote bays (seaward perturbations) whilst blue colours denote horns (shoreward perturbations). The wave conditions are daily-averaged at 10 m depth.*